Lean Complementarity for Poisson Problems

Ruben Specogna

Dipartimento di Ingegneria Elettrica, Gestionale e Meccanica, Università di Udine, Udine 33100, Italy

We introduce a novel technique—lean complementarity—that attempts to eliminate any waste of computational resources occurring during the pursuing of complementarity. First, contrarily to the widely used practice of solving the problem two times with a pair of complementary or complementary-dual formulations, lean complementarity requires just one solution with the computationally cheap formulation based on the scalar potential. This result is enabled by a novel and explicit flux equilibration technique that produces tight bounds and is computationally inexpensive, because no system has to be solved. Second, the systems arising during the adaptive mesh refinement procedure are solved inexactly on purpose, by stopping the iterations of the iterative solver when the algebraic error gets negligible with respect to the discretization error. The discretization error is bounded with complementarity, whereas the algebraic error is computed very accurately with a novel and cheap technique.

Index Terms— **Adaptive stopping criterion for iterative solvers, complementarity, explicit flux equilibration, finite-elements (FEM), fully computable error bounds, hypercircle method, Poisson problem.**

I. Introduction

COMPLEMENTARITY is a rigorous technique to obtain fully computable and guaranteed upper error bounds for system energy [1]—and its related electromagnetic global quantities—in static electromagnetic problems. Such error bounds, which differ from most error estimates presented in the numerical analysis literature by the absence of any generic constant, provide a meaningful stopping criterion for a mesh adaptive refinement, and a robust and physically grounded error indicator—the constitutive error [2]—that suggests where the mesh should be refined. Yet, the standard way of exploiting complementarity is quite costly as it requires to solve the problem two times, for example, with the scalar potential finite element (FEM) formulation [3] and any of its complementary or complementary-dual [4]–[6] counterparts.

It is, therefore, wise to wonder whether faster methods to exploit complementarity exist. Some steps toward this direction, surveyed in Section II, have been already performed. The aim of this paper is to present a cost-effective answer to this question that we call lean complementarity. Lean complementarity is rooted on two novel ideas devised in Section III. First, an explicit flux equilibration technique able to obtain a solenoidal current density from the irrotational electric field produced by the scalar potential formulation $\mathcal{V}$ of a steady-state electric conduction paradigm problem is introduced. Such solenoidal current density is used to bound the error in the dissipated power—i.e., the discretization error—by the classical hypercircle method [1], [7]. Second, we propose an effective method to estimate the algebraic error, which consider that the linear system is not solved exactly at a given iteration of the iterative solver. The idea is to stop iterating with the iterative solver as soon as the algebraic error gets negligible with respect to the discretization error. Finally, Section IV shows some numerical results that demonstrate the effectiveness of lean complementarity.

Manuscript received July 6, 2015; revised August 31, 2015; accepted September 14, 2015. Date of publication September 16, 2015; date of current version February 17, 2016. Corresponding author: R. Specogna (e-mail: ruben.specogna@uniud.it).

Color versions of one or more of the figures in this paper are available online at http://ieeexplore.ieee.org.

Digital Object Identifier 10.1109/TMAG.2015.2479395

II. State of the Art on Complementarity

Taking electrokinetics as a paradigm problem, complementarity requires an irrotational electric field $\mathbf{e}_h = -\text{grad}\upsilon_h$ and a solenoidal current density $\mathbf{j}_h$ satisfying boundary conditions [1], [7], [8]. One may use any $\mathbf{j}_h$ and υ_h that fulfill the aforementioned constraints; however, the resulting bounds would be in general too loose to be of any use. In the literature, in most cases, υ_h is obtained by the FEM scalar potential $\mathcal{V}$ formulation, whereas $\mathbf{j}_h$ is obtained by the vector potential or the mixed-hybrid $\mathcal{H}$ FEM formulations (see [2], [4], [6], [9]). However, we remark that the same results hold irrespectively of the numerical method used to produce υ_h and $\mathbf{j}_h$. On the one hand, the obtained bounds are the tightest possible for a given mesh, as FEM minimizes the energy of the error [3, p. 40] which, in turn, implies that the constitutive error $\Lambda = (1/\sigma)|\mathbf{j}_h - \sigma\mathbf{e}_h|^2$ is minimized [2], where σ is the conductivity assumed elementwise uniform. On the other hand, obtaining $\mathbf{j}_h$, this way is computationally extremely costly, in most cases at least an order of magnitude more costly than obtaining υ_h (see [4], [7], [8]). This renders complementarity less attractive in engineering practice. One stroke complementarity [8] saves the computation of υ_h, since υ_h may be reconstructed from the complementary solution using least squares [4], but the total effort is still dominated by finding $\mathbf{j}_h$.

A. Toward One Stroke Complementarity for $\mathcal{V}$ Formulation

One stroke complementarity is also an option for the cheap $\mathcal{V}$ formulation that provides directly υ_h, whereas the current $\tilde{\mathbf{I}}$ is defined on the faces of the dual complex $\tilde{\mathcal{K}}$ [10] and is there conservative [10], i.e., $\tilde{\mathbf{D}}\tilde{\mathbf{I}} = 0$, where $\tilde{\mathbf{D}} = -\mathbf{G}^T$ and $\mathbf{G}$ is the edge-node incidence matrix [10]. Therefore, the question is whether it is possible to construct, by local manipulations only, a solenoidal current $\mathbf{I}$ defined on the faces of the primal complex $\mathcal{K}$ that produces—once interpolated by face basis functions—a solenoidal current density as close as possible to the one computed by the complementary formulation. A technique to construct such $\mathbf{I}$ is called flux equilibration [11].

For 3-D problems, tight enough bounds are obtained in [12] by solving non-linear programming problems and local systems. Tighter bounds are obtained in [7]

by exploiting the conservativity of $\tilde{\mathbf{I}}$, that is, each dual volume is tessellated with a new (finer) simplicial mesh, and the local corrections are found by solving a Neumann problem on such a refined mesh with a complementary or complementary-dual formulation [7]. This remarkable idea seems to be rediscovered by the numerical analysts [11], and it has become the state of the art nowadays [13]. However, the great majority of papers evaluate the efficiency of this technique by considering 2-D problems. As noticed in [7], for 3-D problems, local systems are not that small, and even if solved in parallel, they require too much time.

A different method, based on an iterative tree technique applied on the primal complex, assumed topologically trivial by hypothesis, has been proposed in [14]. Although computationally efficient, we verified that the obtained bounds are not satisfactory and depend heavily on the choice of the tree.

III. Lean Complementarity

Let us call v the potential solution of the continuous problem, V is the exact solution of the discrete problem with a given mesh, and $V^{(k)}$ is the solution of the discrete problem after the kth iteration of the linear iterative solver. The total error $\eta = v - V^{(k)}$ can be clearly written as the sum of the discretization error $\eta_d = v - V$ and the algebraic error at the kth iteration $\eta_a^{(k)} = V - V^{(k)}$, which vanishes if the system is solved exactly. We neglect the oscillation error term by assuming sources and boundary conditions piecewise uniform in each element.

The stopping criterion for iterative solvers used in lean complementarity is

$$|||\eta_a^{(k)}||| = ||\boldsymbol{\eta}_a^{(k)}||_{\mathbf{K}} < d|||\eta_d||| \tag{1}$$

where $d \ll 1$, $|||\cdot|||$ is the energy norm, $\mathbf{K}$ is the stiffness matrix, $||\cdot||_{\mathbf{K}}$ is the $\mathbf{K}$-norm or discrete energy norm, and $\boldsymbol{\eta}_a^{(k)} = \mathbf{V} - \mathbf{V}^{(k)}$, where $\mathbf{V}$ and $\mathbf{V}^{(k)}$ are the arrays containing the nodal potentials obtained, respectively, as the exact and approximate solutions of the discrete problem. The proposed stopping criterion clearly attempts to balance the two sources of error, as insisting in reducing $||\boldsymbol{\eta}_a^{(k)}||_{\mathbf{K}}$ down to zero would not improve the total error significantly. We have found good results by setting $d = 0.01$. A smaller d would just require a few more solver iterations and would provide only a slightly improved solution.

$||\boldsymbol{\eta}_a^{(k)}||_{\mathbf{K}}$ and $|||\eta_d|||$ in (1) are estimated as follows.

A. Effective Evaluation of the Algebraic Error

The stopping criterion should not be defined—as happens in the usual practice—with the Euclidean norm of the residual $\mathbf{r}^{(k)} = \mathbf{b} - \mathbf{K}\mathbf{V}^{(k)}$, where $\mathbf{b}$ is the right-hand side of the system, or the relative residual $||\mathbf{r}^{(k)}||/||\mathbf{r}^{(0)}||$. The reason why this prescription based on experience may be far from optimal is clear after looking at the relation between $\boldsymbol{\eta}_a^{(k)}$ and $\mathbf{r}^{(k)}$

$$\boldsymbol{\eta}_a^{(k)} = \mathbf{V} - \mathbf{V}^{(k)} = \mathbf{K}^{-1}(\mathbf{b} - \mathbf{K}\mathbf{V}^{(k)}) = \mathbf{K}^{-1}\mathbf{r}^{(k)}. \tag{2}$$

This paper introduces a computationally inexpensive technique to obtain a remarkably precise estimation of $\boldsymbol{\eta}_a^{(k)}$. Let us assume to have just performed the kth iteration of the linear solver, which means that $\mathbf{V}^{(k)}$ is known. Let us run the solver for additional ν iterations, where ν is not fixed but adaptively chosen as the first positive integer for which

$$\mathbf{r}^{(k+\nu)} < c\mathbf{r}^{(k)} \tag{3}$$

holds, where $c \ll 1$. Then, let us consider the difference of the systems at these two stages

$$\mathbf{K}(\mathbf{V}^{(k+\nu)} - \mathbf{V}^{(k)}) = \mathbf{r}^{(k)} - \mathbf{r}^{(k+\nu)}. \tag{4}$$

Since $\mathbf{r}^{(k+\nu)}$ is negligible with respect to $\mathbf{r}^{(k)}$ thanks to (3), (4) becomes (2), and therefore, the solution $\boldsymbol{\eta}_a^{(k)}$ of (2) can be approximated by $\mathbf{V}^{(k+\nu)} - \mathbf{V}^{(k)}$.

At iteration k, also the discretization error $\boldsymbol{\eta}_d$ is estimated, as proposed in Section III-B. Then, if stopping criterion (1) is fulfilled, solver iterations are stopped. Otherwise, k is set to $k + \nu$, and solver iterations continue until (3) is verified again. We have found good results by setting $c = 0.1$. For such c, ν turned out to be always 2 in the example presented in Section IV. A smaller c would just slightly improve the accuracy of $\boldsymbol{\eta}_a^{(k)}$ at the price of increasing ν.

We remark that Galerkin orthogonality [3, p. 40] does not hold at a given iteration of the linear solver, which means that the energy of the algebraic error is not the error in energy (or, as in our problem, in the dissipated power).

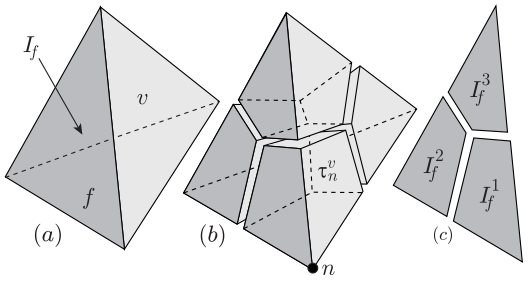

Fig. 1. (a) Tetrahedron v. Current I_f associated with face f (highlighted in the picture). (b) v is partitioned in four dual volume portions. (c) I_f over face f is obtained as $I_f^1 + I_f^2 + I_f^3$.

B. Bounding the Discretization Error With an Explicit Flux Equilibration Technique

We use the classical hypercircle method [1], [7], [13] to produce a guaranteed bound for $|||\eta_d|||$ through a novel and fast flux equilibration technique.

Let us first assume that the system is solved exactly, i.e., $\tilde{\mathbf{D}}\tilde{\mathbf{I}} = \mathbf{0}$ holds. Let us consider an element v of the mesh [see Fig. 1(a)]. Let us also define the portion τ_n^v of dual volume $\tilde{v}$ (dual to node n) inside the element v as $\tau_n^v = v \cap \tilde{v}$ [see Fig. 1(b)]. The idea is to construct a current that is solenoidal in each portion of dual volume. If so, it is solenoidal also in the initial tetrahedral mesh, as the current continuity law on v is a linear combination of continuity laws on its four dual volume portions. Then, $\mathbf{I}$ is constructed by assembling exactly three contributions for each face [see Fig. 1(c)].

To obtain a solenoidal current in dual volume portions, one may solve a Neumann problem on the refined mesh of $\tilde{v}$ with a current conservative formulation. Even if such local systems are smaller than the ones in [7], their solution requires an

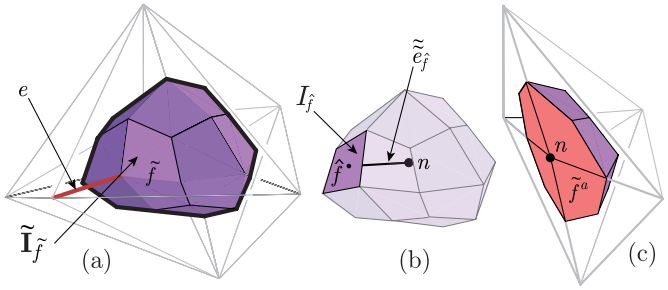

Fig. 2. (a) Dual volume $\tilde{v}$ and a dual face $\tilde{f} \in \partial\tilde{v}$. (b) Portion of dual face $\hat{f} \in \partial\tilde{v}$ and its associated current $I_{\hat{f}}$. Edge $\tilde{\tilde{e}}_{\hat{f}}$ dual to $\hat{f}$ is also shown. (c) If $n \in \partial\mathcal{K}$, $\tilde{v}$ is closed by the additional dual face $\tilde{f}^a$.

unacceptable amount of time, and it is, therefore, mandatory to devise an explicit technique.

The key idea at the ground of the novel flux equilibration technique is that $\tilde{v}$ is a polyhedron whose (flat) faces are the portions of dual faces. Let us consider a portion of dual face $\hat{f} \subset \partial\tilde{v}$ ($\hat{f}$ also denotes the face vector of the portion of dual face) [see Fig. 2(b)] and let us call $I_{\hat{f}}$ the current associated with $\hat{f}$. Such currents are constructed element by element by multiplying the edge elements mass matrix by the vector of electromotive forces on the primal edges (see [7]). By considering such a polyhedron, one has

$$|\tilde{v}|\mathbf{I}_3 = \sum_{\forall \hat{f} \in \partial\tilde{v}} \tilde{\tilde{e}}_{\hat{f}} \otimes \hat{f} \tag{5}$$

see [15], where $\otimes$ denotes the tensor product of two vectors, $\mathbf{I}_3$ is the identity matrix of dimension three, $|\tilde{v}|$ is the volume of $\tilde{v}$, and $\tilde{\tilde{e}}_{\hat{f}}$ is the edge vector of an edge dual to $\hat{f}$ [see Fig. 2(b)]. We remark that edges as $\tilde{\tilde{e}}_{\hat{f}}$ are not classical dual edges, but they are dual of dual face portions as $\hat{f}$. Let us now multiply both sides of (5) by a current density $\mathbf{J}$, uniform in $\tilde{v}$ by hypothesis

$$|\tilde{v}|\mathbf{J} = \sum_{\forall \hat{f} \in \partial\tilde{v}} \tilde{\tilde{e}}_{\hat{f}} \otimes \hat{f}\mathbf{J} = \sum_{\forall \hat{f} \in \partial\tilde{v}} \tilde{\tilde{e}}_{\hat{f}} (\hat{f} \cdot \mathbf{J}). \tag{6}$$

We require $\mathbf{J}$ to be uniform, because then it is also *solenoidal* in $\tilde{v}$. The normal component of $\mathbf{J}$ (i.e., $I_{\hat{f}} = \hat{f} \cdot \mathbf{J}$) is continuous across ∂v. Thus, $\mathbf{J}$ inside $\tilde{v}$ shall be constructed as

$$\mathbf{J} = \frac{1}{|\tilde{v}|} \sum_{\forall \hat{f} \in \partial\tilde{v}} I_{\hat{f}} \tilde{\tilde{e}}_{\hat{f}}. \tag{7}$$

We remark that $\mathbf{J}$ in (7) can be computed by assembling contributions elementwise. Thanks to the divergence theorem, the current obtained by integrating $\mathbf{J}$ on the faces in the boundary of each dual volume portions is solenoidal.

Dual volumes dual to nodes $n \in \partial\mathcal{K}$ are treated in the same way, but they require two additional details. First, there is the need to assign in the best possible way the flux on the additional boundary dual face $\tilde{f}^a$ [see Fig. 2(c)], which is part of $\partial\tilde{v}$. That is, if a Neumann boundary condition has to be applied on a portion of $\tilde{f}^a$, its flux is computed by integrating the Neumann data. Otherwise, in the case of Dirichlet boundary condition, the flux is obtained by integrating $\sigma\mathbf{e}_h$. Second, the node used for the construction of $\tilde{\tilde{e}}$ edges cannot be n anymore, since n is on the boundary of the polyhedron. Therefore, in this case, the center of the polyhedron $\tilde{v}$ is used.

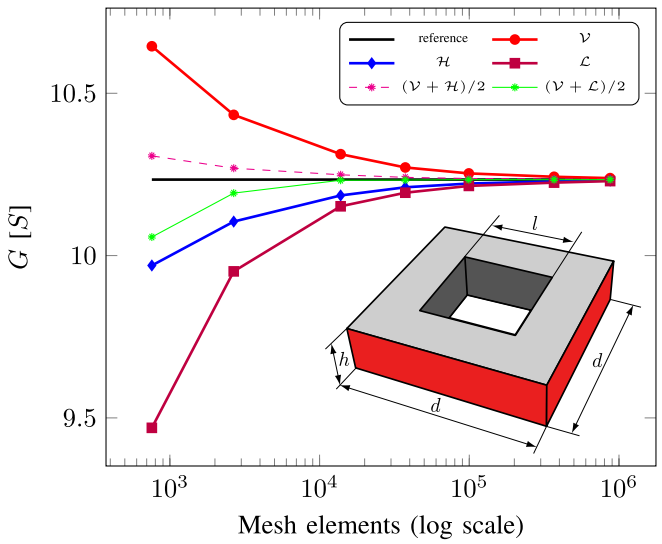

Fig. 3. Geometry of the square resistor and convergence of the conductance value with respect to an increasing number of mesh elements.

Yet, the proposed approach is, in general, not resolutive, as the obtained current $\mathbf{I}$ is, in general, only quasi-equilibrated. This happens always in the first iterations of the iterative solver, as $\tilde{\mathbf{D}}\tilde{\mathbf{I}} = \mathbf{0}$ does not hold yet. This may also happen when $\tilde{v}$ is not star shaped (in the few places where the domain has a sharp reentrant corner), since (5) holds only for star-shaped polyhedra. Both issues are solved by applying a technique similar to [14] to the quasi-equilibrated current. Thus, at the end, the resulting current is solenoidal up to machine precision.

IV. Numerical Experiments

We present the results on a benchmark consisting of a square resistor [see Fig. 3] ($h = 1$ m, $d = 4$ m, and $l = 2$ m) and [4]. We considered this simple benchmark because a reference solution is available, and because it exhibits strong corner singularities that yield to a poor convergence if adaptivity is not used. Various formulations to solve each electrokinetic problem arising during the adaptive mesh refinement have been compared. $\mathcal{V}$ and $\mathcal{H}$ indicate the results obtained by FEM scalar potential and mixed-hybrid formulations, respectively, whereas $\mathcal{L}$ the ones obtained with the novel flux equilibration technique. The novel stopping criterion has been implemented in the AGgregation-based algebraic MultiGrid solver [16], and all simulations have been performed on a laptop with 16 Gb of RAM.

Fig. 3 compares how the conductance computed by the various techniques converges to the exact solution (reference) when the number of elements is adaptively increased. In Fig. 3, $(\mathcal{V}+\mathcal{H})/2$ and $(\mathcal{V}+\mathcal{L})/2$ represent the conductance values obtained by averaging the conductances produced by $\mathcal{V}$ and $\mathcal{H}$ or $\mathcal{V}$ and $\mathcal{L}$, respectively.

To better investigate the effectiveness of lean complementarity, let us consider the last and most expensive simulation solved during the adaptive mesh refinement.

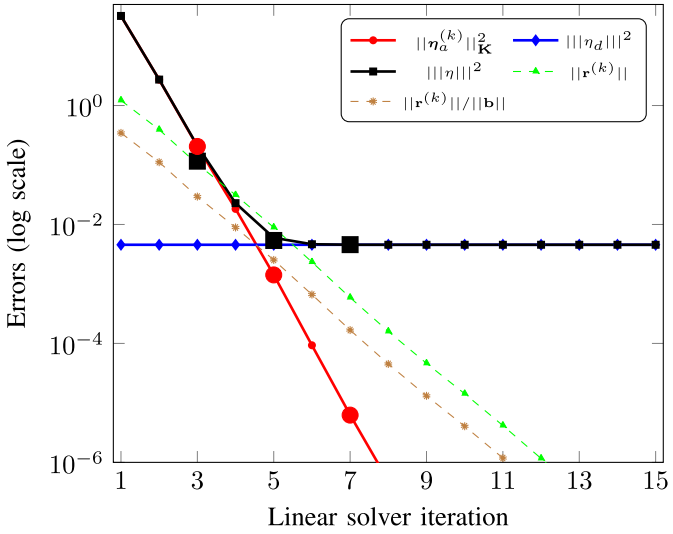

Fig. 4. Continuous lines: exact values of $||\boldsymbol{\eta}_a^{(k)}||^2_{\mathbf{K}}$, $|||\eta_d|||^2$, and $|||\eta|||^2$ in logarithmic scale for the final adapted mesh. Bigger marks: same quantities estimated by lean complementarity at iterations 3, 5, and 7. The residuals $||\mathbf{r}^{(k)}||$ and the relative ones are also shown.

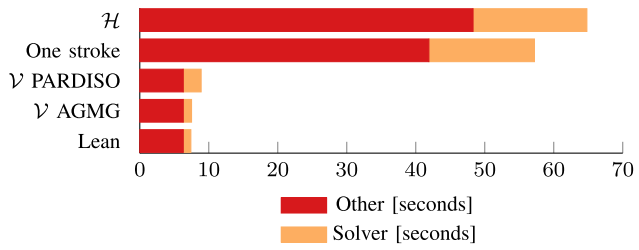

Fig. 5. Total wall time required to simulate the problem on the final adapted mesh. Solver represents the time in seconds spent in the solution of the linear system. Other considers the time spent in all other parts as matrix assembling and pre- and post-processing.

The mesh is formed by 889 350 tetrahedra and 157 239 nodes. Continuous lines in Fig. 4 represent the exact values of $||\boldsymbol{\eta}_a^{(k)}||^2_{\mathbf{K}}$, $|||\eta_d|||^2$, and $|||\eta|||^2$. The exact value of $\boldsymbol{\eta}_a^{(k)} = \mathbf{V} - \mathbf{V}^{(k)}$ has been computed using the solution $\mathbf{V}$ obtained with the direct solver Intel MKL PARDISO. Bigger marks represent the same quantities estimated very accurately by lean complementarity at iterations 3, 5, and 7. Therefore, flux equilibration and the estimation of $||\boldsymbol{\eta}_a^{(k)}||_{\mathbf{K}}$ have been performed only three times. The picture also shows the absolute residuals $||\mathbf{r}^{(k)}||$ and the relative ones. Always by considering the last and most expensive simulation, the multigrid solver is stopped at iteration 7 by stopping criterion (1), whereas the classical stopping criterion (relative residual set to 10^{-8}) performs 15 iterations. Since it requires half multigrid iterations, lean complementarity results slightly faster than the $\mathcal{V}$ formulation with the classical stopping criterion [see Fig. 5] even though the latter cannot exploit complementarity. We also remark that the AGMG solver is always much faster than direct solvers as PARDISO. On the considered mesh, PARDISO is 2.2 times slower (1.2 versus 2.6 s), but the difference grows fast with mesh density. In the proposed benchmark, PARDISO is about 6.3 times slower for a mesh consisting of ∼1.7 million nodes (16 versus 100 s) and 14 times slower for 2.7 millions nodes (25 versus 351 s). Moreover, the memory required by PARDISO grows rapidly, and it becomes an insurmountable obstacle for solving industrial-sized problems.

The efficiency of lean complementarity on more complicated benchmarks and a thorough cost-effectiveness analysis with respect to high-order methods is an ongoing work. For 2-D problems, the evaluation performed in [17] shows that even the standard way to exploit complementarity (i.e., solving two global systems for each mesh) compares favorably with respect to the second-order FEM, especially if corner singularities are present and if one does not require an accuracy much greater than the uncertainty of material parameters.

ACKNOWLEDGMENT

R. Specogna is partially supported by PAR FSC 2013 EMCY project of Friuli Venezia Giulia region, Italy.

REFERENCES

[1] J. L. Synge, *The Hypercircle in Mathematical Physics*. New York, NY, USA: Cambridge Univ. Press, 1957.
[2] J. Rikabi, C. F. Bryant, and E. M. Freeman, "An error-based approach to complementary formulations of static field solutions," *Int. J. Numer. Methods Eng.*, vol. 26, no. 9, pp. 1963–1987, 1988.
[3] G. Strang and G. Fix, *An Analysis of the Finite Element Method*. Englewood Cliffs, NJ, USA: Prentice-Hall, 1973.
[4] R. Specogna, "One stroke complementarity for Poisson-like problems," *IEEE Trans. Magn.*, vol. 51, no. 3, Mar. 2015, Art. ID 7401404.
[5] R. Specogna, "Diagonal discrete Hodge operators for simplicial meshes using the signed dual complex," *IEEE Trans. Magn.*, vol. 51, no. 3, Mar. 2015, Art. ID 7400904.
[6] Z. Ren and X. Xu, "Dual discrete geometric methods in terms of scalar potential on unstructured mesh in electrostatics," *IEEE Trans. Magn.*, vol. 50, no. 2, Feb. 2014, Art. ID 7000704.
[7] A. Bossavit, "A posteriori error bounds by 'local corrections' using the dual mesh," *IEEE Trans. Magn.*, vol. 35, no. 3, pp. 1350–1353, May 1999.
[8] A. Bossavit, "Mixed-hybrid methods in magnetostatics: Complementarity in one stroke," *IEEE Trans. Magn.*, vol. 39, no. 3, pp. 1099–1102, May 2003.
[9] R. Specogna, "Complementary geometric formulations for electrostatics," *Int. J. Numer. Methods Eng.*, vol. 86, no. 8, pp. 1041–1068, 2011.
[10] A. Bossavit, "How weak is the 'weak solution' in finite element methods?" *IEEE Trans. Magn.*, vol. 34, no. 5, pp. 2429–2432, Sep. 1998.
[11] R. Luce and B. I. Wohlmuth, "A local a posteriori error estimator based on equilibrated fluxes," *SIAM J. Numer. Anal.*, vol. 42, no. 4, pp. 1394–1414, 2004.
[12] G. Marques, S. Clénet, and F. Piriou, "Error estimators in 3D linear magnetostatics," *IEEE Trans. Magn.*, vol. 36, no. 4, pp. 1588–1591, Jul. 2000.
[13] M. Vohralík, "A posteriori error estimates for efficiency and error control in numerical simulations," Univ. Pierre Marie Curie, Paris, France, Lecture Notes Course NM497, Feb. 2015.
[14] F. Marmin, S. Clénet, F. Bouillault, and F. Piriou, "Calculation of complementary solutions in 2D finite element method application to error estimation," *IEEE Trans. Magn.*, vol. 36, no. 4, pp. 1583–1587, Jul. 2000.
[15] L. Codecasa, R. Specogna, and F. Trevisan, "A new set of basis functions for the discrete geometric approach," *J. Comput. Phys.*, vol. 229, no. 19, pp. 7401–7410, 2010.
[16] Y. Notay. (2012). *AGMG Aggregation-Based Algebraic Multigrid Software*. [Online]. Available: http://homepages.ulb.ac.be/~ynotay/agmg
[17] R. Specogna, "Extraction of vlsi multiconductor transmission line parameters by complementarity," *IEEE Trans. Very Large Scale Integr. (VLSI) Syst.*, vol. 22, no. 1, pp. 146–154, Jan. 2014.